



Photocatalytic degradation of benzotriazole: by-products, bio-toxicity and kinetic study

Samira Moslemi^a, Hamidreza Nassehinia^b, Ayat Rahmani^{b,*}

^a*Environmental Health, Department of Environmental Health, Semnan University of Medical Sciences, Semnan, Iran, Tel. +98 2335220132; email: moslemisamira@yahoo.com (S. Moslemi)*

^b*Research Center for Health Sciences and Technologies, Semnan University of Medical Sciences, Semnan, Iran, Tel. +98 9333900151; email: ayat_rahmani@yahoo.com (A. Rahmani), Tel. +98 23352201; email: hamidrezanassehi@gmail.com*

Received 30 August 2021; Accepted 9 November 2021

ABSTRACT

Benzotriazoles (BTAs) are high production volume substances that are widely used in various industrial processes and in households. In this study, the photocatalytic and photolysis degradation of benzotriazole was studied on the TiO₂ nanoparticles coated on the fixed bed, which was treated in two light sources including UV_C (250 nm) and natural solar in quartz glass tubes fitted with design compound parabolic concentrators (CPC). The effects of samples kinetic reaction, TOC and COD removal, by-products and bio-toxicity were evaluated. Characterization of the TiO₂ nanoparticles samples was performed by FE-SEM, XRD, UV-VIS spectrophotometer, and BET measurements. The highest photocatalytic and photolysis activity for the degradation of BTA has been obtained for the TiO₂/UV_C and UV_C whit 99% and 45 efficiencies in 120 min. Also, the highest photocatalytic and photolysis activity for the degradation of BTA has been obtained for reactor CPC and 84% and 36% efficiency in 120 min. The photocatalytic degradation reaction of BTA was monitored by HPLC, TOC, and GC-MASS analyses. The GC-MASS analysis results indicate that degradation of BTA occurs through products triazole, tolyltriazole and anilin were identified ring cleavages followed by subsequent reactions with OH radicals. The metabolites show toxic effects, but they are not as toxic as benzotriazole, resulting in a general decrease in toxicity as a result of photocatalytic degradation.

Keywords: Photocatalytic and photolysis degradation; Benzotriazole; Compound parabolic concentrators; Solar; TiO₂; UV_C

1. Introduction

Benzotriazole (BTA) and its derivatives have extensive applications as lubricant and polymer stabilizers, pesticides and components of photographic developers. The impact of these substances on the environment is made greater by their resistance to biological degradation, this confines the choice of purification methods to the fled of chemical treatments [1,2]. In addition, the elimination of these compounds using conventional treatment processes appears to be poor that only 37%–62% of BTA can be removed by conventional

treatment processes [3]. Also, due to their relative resistance to biodegradation, BTA is removed only the partial amounts of BTA in mechanical–biological treatment units [4]. Advanced oxidation processes (AOP) are very attractive for the development of treatment methods capable of complete destruction of toxic substances which are refractory to biological degradation [5,6]. These processes are based on the use of thermodynamically strong oxidants (O and the application of promoting, (H₂O₂) devices (UV, catalyst addition) which increase their reactivity to levels allowing complete pollutants abatement at suitable treatment times

* Corresponding author.

[7–9]. AOP techniques are quite promising for the application on both a small and large scale, so they could also be applied to solve very specific treatment problems [10]. The reactive oxygen species can not only destroy an enormous variety of chemical contaminants in water but also reason fatal damage to microorganisms. The photocatalytic properties of numerous semiconductors had been investigated (TiO_2 , ZnO , Fe_2O_3) [11,12]. Among these, the most commonly used for water treatment applications are titanium dioxide (TiO_2) and zinc oxide (ZnO). TiO_2 and ZnO were the wideband semiconductors whose bandgap energy of 3.2 and 31.3 eV corresponds to photons of wavelength shorter than 400 nm. If the interest is the solar application, materials active in the visible range are desirable [13–16].

The purpose of this study is to assess the feasibility of the photocatalytic and photolysis degradation of benzotriazole in the presence of fixed-bed TiO_2 . For this purpose, TiO_2 nanoparticles were coated on a fixed bed treated with two light sources; that is, UV_C (250 nm) and solar light. Characterization of the fixed bed TiO_2 samples was performed by FE-SEM, XRD, UV-VIS spectrophotometer, and surface area (BET) measurements. The degradation reaction was also followed by HPLC and GC-MAS analyses.

2. Material and method

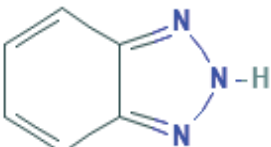
2.1. Materials and reagents

BTA (purity 99.99%), methanol, titanium dioxide (TiO_2 99/5%-CAS: 1317-700(Rutile (TiO_2)) hydrofluoric acid, water grade HPLC were purchased from Merck, Germany. Molecular structure of BTA in non-hydrolyzed form is illustrated in Table 1.

2.2. Preparation of TiO_2 nanocatalyst

First, to create a higher effective surface on the glass, the glass surface was placed in contact with 30% fluoride acid for 50 min. The glass beds were washed with distilled water and then they were set in the plastic containers contain NaOH 1 normality for 50 min. For making the TiO_2 solution, the TiO_2 powder with 99.8% purity was prepared and the solution with 3% TiO_2 was made. In the next step, the solution is placed in an ultrasonic (sono plus HD 2070-HD2200) apparatus at 50°C for 90 min to obtain a homogeneous mixture. After distributing this homogeneous suspension on the glass surface, it was placed at a normal temperature for 3–4 h. After this period of time, the amount of water remaining on the residual glass surface

Table 1
Molecular structure of benzotriazole

Molecular formula	$\text{C}_6\text{H}_5\text{N}_3$
Molecular structure	
Molecular weight	119.12 g/mol
Maximum wavelengths	465 nm

was removed and the sample was placed at a normal temperature for 24 h to dry again. After this step, the glass was placed in the furnace for 1 h and a half and the temperature gradually increased from 50°C to 500°C to create the calcification of the nanoparticles on the substrate surface.

2.3. Reactor setup

In this study, we used 3 batch reactors and Dimensions and properties of the quartz glass tube fitted with reactors 1 and 2 (Table 2). At first the glass reactor 1 was designed (29 cm × 20 cm × 10 cm), then glass bed coated with TiO_2 was placed at the bottom of the reactor and a radiation source was located above the reactor using a UV lamp (Philips UV-C Lamp 8 W), reactor 2 with the same design was used Solar light has been used as a light source in the photocatalytic process.

Reactor3, (compound parabolic concentrator (CPC) mirror), (Fig. 1a), for increasing the intensity of the radiation was received, (CPC) mirror was designed (Table 2). Collection parallel beam at an angle to the axis of symmetry CPC is the highest angle of divergence for light collected by the reflection on a different part of the point on the center of their F. Reactor used in this study (CPC) mirror with a diameter of 100 cm and a length of 150 cm, which able to reflex more sunlight to a focal point (F). This is studying the reflective surface of the CPC consist of, which reflects 86% of UV radiation and 96% of other types of solar radiation. Quartz glass tube containing water in height 7.5 cm from the center of the reactor, the F has placed mirrors reactor to the North-South and at an angle of 35° to 15° considering region and the season are placed sampled.

The dimensions of the quartz glass tube that was used in this study were 150 cm in length, 5 cm in outer diameter,

Table 2
Dimensions and properties of the quartz glass tube fitted with reactors 1and 2

		Length (cm)	Width (cm)	Aperture area (m^2)	Thickness (mm)	Diameter (cm)	Treated volume (L)
Reactor 1	CPC	150	100	0.38	2	100	
	Glass tubes	150	100		1.5	5	3.2
	Black copper	100	3	0.03	1		
Reactors 2 and 3		30	16				1

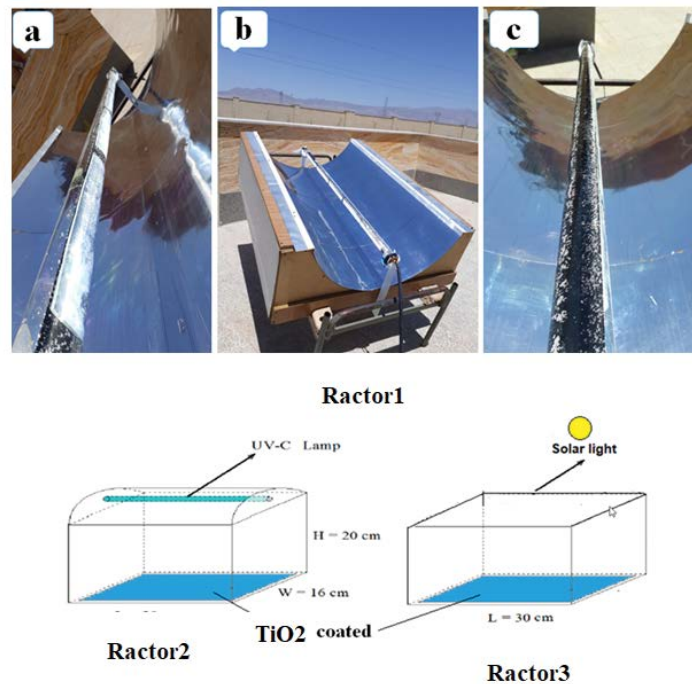


Fig. 1. Photographs showing the quartz glass tube fitted with black copper in the reactors CPCs filled with sample during real sunlight exposure (Reactor 1 a,b,c), and schematic of reactors 2 and 3.

1.5 mm in wall thickness, and 2.95 L internal volume, (Fig. 1b). The glass tubes can have transmitted 93% and 50% of UVA and UVB light, respectively. In this study, an aluminum metal with black color was used as a superconductor which was able to accelerate and increase the rate of thermal energy for removal of BTA. then glass beds that were horizontally coated with TiO_2 were fixed with aluminum that was located in the center of the glass tube (aluminum metal was placed vertically to absorb lighter). The accurate position of the tube was on the focus (F) of the mirror CPC.

2.4. Characterization techniques

In order to the measurement of size and image of nanoparticles of catalyst, we used x-ray diffraction (XRD) and scanning electron microscope (SEM) respectively.

2.5. Experimental

In this study, we used to stoke 1,000 mg/L powder of BTA for preparing the test solutions. For obtaining peak time and a calibration curve we were prepared standard concentrations (10, 20, 30, 40, 50, and 60 mg/L) from the stoke sample. Then the samples of BTA dosage (1, 5, 10, 15, 20 and 40 mg/L from stoke that reached 1,000 mg/L by distilled water) were poured into the reactor.

2.6. Analytical methods

2.6.1. HPLC analysis

HPLC was used to measure residual concentrations in samples. The solutions were prepared as standard

concentrations (1, 20, 40, 60, 80 mg/L) from the stoke sample to obtain peak time and a calibration curve. Finally, After Sunlight emission and UVc at a wavelength of 254 nm at specified times, the sample was transmitted to the HPLC apparatus for analysis. The flow rate of 1 ml/min for the mobile phase, which consisted of methanol and water (70:30 v/v) wavelengths used for the quantification of the BTA were: 275 nm. The removal efficiency (R) of BTA was calculated by the following equation:

$$R = \frac{(C_0 - C_e)}{C_0} \times 100 \quad (1)$$

where R is the removal efficiency (%), C_0 the initial concentration of BTA (mg/L), and C_e is the concentration in equilibrium of BTA (mg/L).

2.6.2. GC/mass analysis

In order to evaluate the efficiency of removal of BTA were used the GC/mass. For preparation the samples for testing 10 cc from samples after irradiation times that were filtered with 1 cc chloroform and 4 cc methanol were mixed in falcon tube that made of polyethylene, and placed in a centrifuge machine with 3,500 rpm for 30 min; then, 1 cc of the solution in the separated phase was taken from the surface and injected into the GC/mass. All experiments were conducted in laboratory conditions at $25^\circ\text{C} \pm 2^\circ\text{C}$.

2.7. Reaction kinetics

In this study, Eq. (2) was used to calculate the reaction kinetics.

$$\ln \frac{C}{C_0} = -kt \quad (2)$$

where C_0 is the initial concentration and C is the concentration of the wastewater. t is the solution contact time in the reactors and k is the reaction speed constant.

2.8. TOC and COD test

For measuring total organic carbon (TOC) for mineralization, 10 cc of the sample after the reaction time of 120 min, was taken and after injecting 0.1 cc HCl 1 normal, the NPOC content of the sample was measured by the TOC meter machine at 800°C furnace temperature. The model of the device was Jena-C3100 made in Germany. The model of the device was Jena-C3100 made in Germany [17]. The chemical oxygen demand (COD) was measured by open reflex methods [18].

2.9. BTE test

In order to establish an effective surface of nanoparticles in both powdered forms and after coating conditions were used The BTE Machin. In this study, the TiO_2 sample was first prepared in powder form before coating, and then the nanoparticles after coating were prepared to test the effective surface area.

2.10. Toxicity test

Toxicity analysis of Microtox is one of the most promising rapid methods for biological monitoring of the environment. The purpose of this test is to measure the toxicity of benzotriazole and metabolites using the Microtox t toxicity test using *Vibrio fischeri*. Bacterial growth pattern in photobacterium broth culture medium was determined by measuring cell density at 600 nm and it was found that the optimal bacterial growth time was about 16–16 h after inoculation. In this study, samples are tested in a period of 0–120 min from Reactor 1 to test the toxicity of benzothiazole and the effect on *Vibrio fisher* bacteria in the Microtox test due to limitations in the nitrification process.

2.11. Solar experiment

This study was conducted under natural solar radiation at the Damghan-Iran that geographical location, 3 min at 25° to 39° and 47 min north latitude and 44°, 63°, 18 min east longitude 5 min and which has a very good position to use solar energy. experiments began at 10 am and finished at 5 pm local time. samples (5, 10, 15, 20 and 40 mg/L BTA) were collected after 15, 30, 45, 60, 90 and 120 min of solar exposure and then filtered for HPLC to evaluate the efficiency of removal of BTA. reactor to the North–South and at an angle of 35° to 15° considering region and the season are placed sampled. Solar and UV irradiance was measured with a global UV radiometer (295r (2 nm UV and 400–1,500 nm Solar, Model HAGNER, Sweden). The primary temperature of all samples was about 46°C ± 11°C.

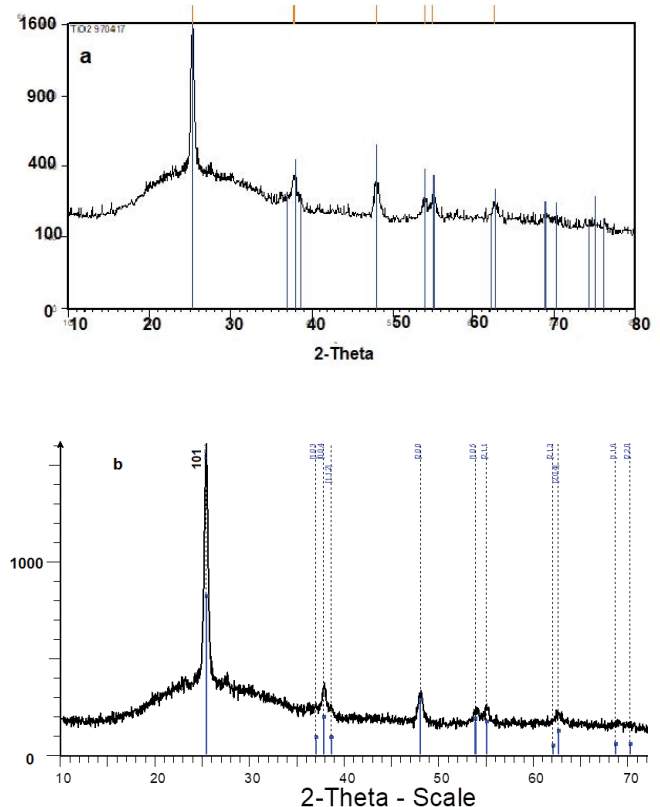


Fig. 2. XRD diffractograms for TiO_2 samples after coating (a), before coating (b).

3. Results and discussion

3.1. Characterization of the nanocatalyst

The results of the XRD of powdered nanoparticles and the layer coated on the glass substrate are shown in Fig. 3.

In XRD results, both molecular phases of nanoparticles are calculated to be 79% anatase and 24% rutile. Also, the anatase peak number (101) has a large consistency with the angle before the coating. The comparison of the anatase and rutile phase before and after the nanoparticle coating showed that the coating process, which was carried out at 550°C in the vacuum furnace, did not change the structure of the nanoparticle (Fig. 2). The results of the BET test presented in Table 3 show that during the coating process, the size of nanoparticle crystals has increased from 21 nm in a powdery state to 34 nm after the coating. Changing the size of the nanoparticle crystal can be caused by the high calcification on the surface of the glass substrate.

In Fig. 3a, FESEM shows the surface of the glass substrate before coating, which caused the contact of the substrate with HF and corrosion on the glass surface to provide a suitable substrate for the nanoparticle coating. Fig. 3b shows the substrate after coating that the nanoparticle is uniformly distributed over the entire surface.

Moreover, Fig. 3b shows the size of the particles in the indicated layer. After the coating process, the size of the crystals is larger than the powdery state. The effective surface of the nanoparticle is 51.4 m^2/g in powder

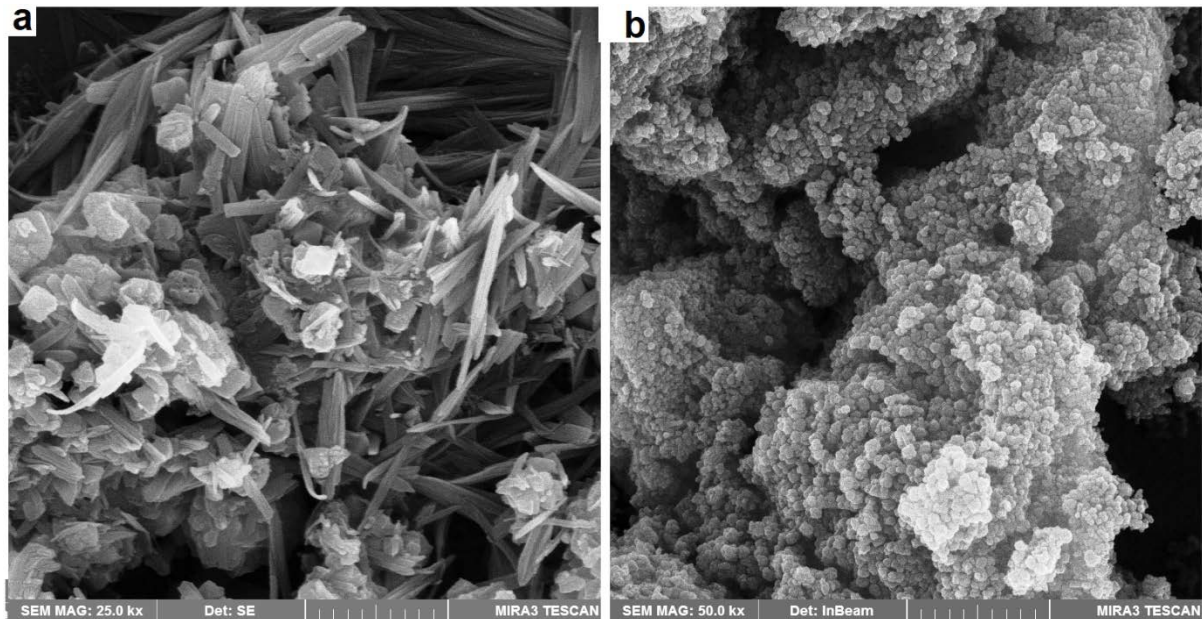


Fig. 3. FESEM surface of the glass substrate before coating (a), after coating with TiO_2 (b).

form (Table 3). After the coating, the effective surface of nanoparticles decreased to $48.8 \text{ m}^2/\text{g}$, probably due to the calcification process during the coating process [5]. In this study, the UV absorption rate by nanoparticles was investigated at a wavelength range of 200–1,000 nm by UV-Vis diffuse reflectance spectroscopy (DRS). The results of this analysis show that the highest UV absorption is at 250 nm wavelength in the UV_C wavelength range. The nanoparticle also has a maximum absorption rate at wavelengths of 320–360 nm, which are located in the UV_A wavelength range. This nanoparticle has a very low absorption at wavelengths higher than 400 nm, which is in the range of the visible light of the sun [19].

3.2. Solar light

The essays were carried out on sunny days without cloud cover. Fig. 4 shows the peak sun hours of 11.30 to 14.30, so tests were done at the same time. The maximum Solar light and UV radiations were 800 and 33.4 W/m^2 respectively (Fig. 4).

3.3. Photolysis degradation of BTA

Fig. 5 shows the photocatalytic degradation of benzotriazole with three reactors, reactor1 (UV_C 250 nm), reactor 2 (CPC) and reactor 3 (solar light). It is noticed that the highest rate of photolysis in the Reactor1 is 45% after 120 min UV irradiation to the fact that the maximum absorption of UV is at wavelengths of 255–280 nm by benzotriazole, the amount of the benzotriazole is broken down and converted to by-product materials [20].

The effect of sunlight on each solar Reactor2 whit irradiance $3,500 \text{ W/m}^2$ and UV-A 145 W/m^2 is 36% and in Reactor 3 whit irradiance 700 W/m^2 and UV-A 30 W/m^2 14%. The amount of UV absorption by benzotriazole is negligible

at wavelengths over 340 nm, which can prevent the degradation of benzotriazole by sunlight over short periods of time. The study of Felis et al. [20] was shown that benzotriazole is resistant to UV-A and does not degrade by photolysis. The other investigated substance, BTA, was not significantly degraded by the sunlight. After 660 min of the irradiation (irradiance $\frac{1}{4} 1,000 \text{ W/m}^2$), only 26% BTA removal was observed. It was a significantly lower removal of BTA, in comparison to the results obtained by the other authors [21–23].

3.4. Photocatalyst degradation of BTA

In the photocatalytic process in the benzotriazole degradation, three methods of Reactor 1, 2 and 3 were investigated. The highest removal efficiency in the photocatalytic process in Reactor 1 was 99% after 120 min of contact. The removal efficiencies in Reactors 2 and 3 after 120 contacts were 97% and 70%, respectively. The most important factor in the degradation of benzotriazole in the presence of free radicals of OH^\bullet resulting from the photocatalytic process. As shown in Fig. 6 the TiO_2 nanoparticles absorption is at 254 wavelengths at the UV_C range and, in fewer wavelengths, 321 nm in the wavelength of the UV_A of the sun, in conclusion it can be said that Reactor 1 is capable of producing more free radicals resulting in higher efficiency in benzotriazole removal.

Comparing two solar reactors, the CPC reactor, which is a light concentrator, has higher efficiency and coefficient k than reactor 3, which is a conventional solar reactor. The reason for this difference is two factors: the intensity of light irradiation and temperature rise. As shown in Fig. 4 the intensity of IR and UV_A in the CPC are irradiance $3,500$ and 145 W/m^2 , respectively. In the solar reactor 700 and 30 W/m^2 , respectively. As shown in previous studies, the increase in the intensity of light radiation, especially at wavelengths of

Table 3
Crystallite sizes, surface areas, band gap energies Eg and absorption wavelengths for the TiO₂ samples

	BET (m ² /g)	Cristal size (nm)	Purity (%)	Eg (eV)	UVc (Max absorption)	Solar light (Max absorption)
TiO ₂	51.4	21	99.5	3.02	250 nm	320 nm
TiO ₂ (coating)	48.8	34	99.4	3.01	250 nm	320 nm

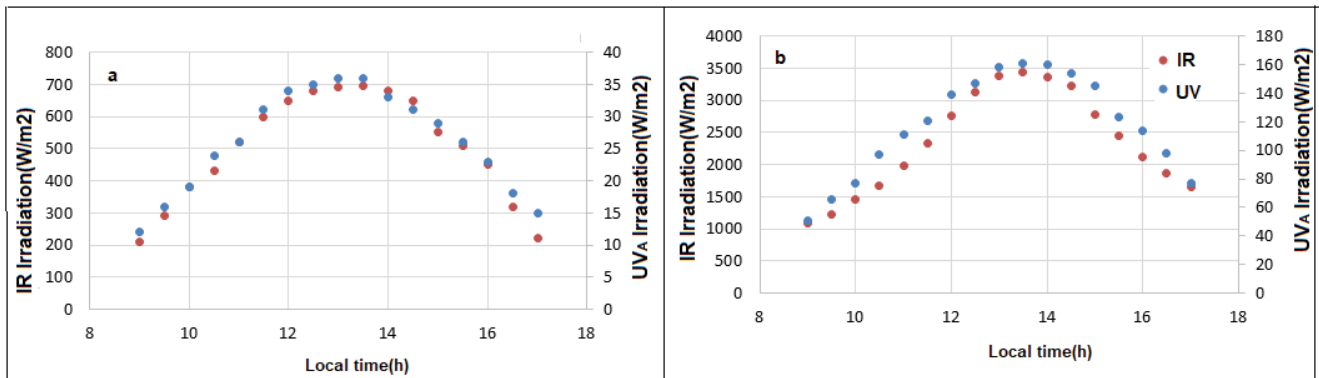


Fig. 4. Graphic representations of the values of solar UV and solar irradiance radiations registered during the degradation, Solar (a) and CPC (b).

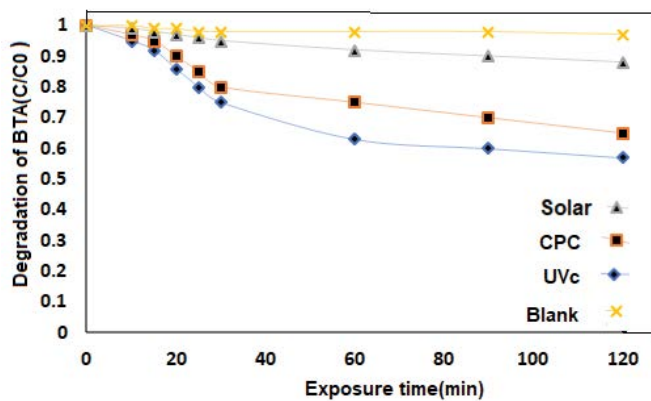


Fig. 5. Effect of solar solar, CPC and UVc on photolysis degradation of benzotriazole.

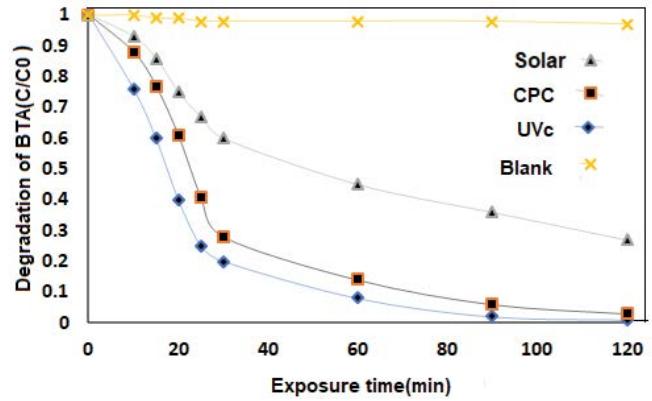


Fig. 6. Effect of solar, CPC and UVc on photocatalytic degradation of benzotriazole.

300–350 nm, grows the efficiency of the photocatalytic process and the production of free radicals that are effective in removing benzotriazole [20]. Also, benzotriazole remains stable at temperatures below 90°C, but the rise in temperature from 20°C to 90°C is effective in the photocatalyst process and free radical production [24].

3.5. Kinetic reaction of BTA

Photolysis in 280 nm and OH[•] oxidation are two mechanisms that contributed to the degradation of BTA. Fig. 7 shows the kinetic reaction of BTA at a time of min. It can be seen that the kinetic reaction of photolysis in benzothiazole solution, which is contacted with a UV lamp (254) is 0.08 at 30 min. The kinetic reactions in the photocatalytic process in the reactor 1, reactor 2, and reactor 3 are 1.21,

1.09, and 0.34, respectively, at 30 min. Overall, the reason for increasing the reaction rate in reactor 1 is due to production of higher OH[•] radical than other reactors.

The reaction speed of the Reactors 2 and 3, which used solar radiation at wavelengths of more than 300 nm, as a solar source in the photocatalytic process, is lower than the Reactor 1, the main reason for this difference is that the most absorbing light TiO₂ is at 254 nm wavelength and has a lower light absorption at the wavelength of the sunlight, resulting in a lower free radical of OH[•] in Reactors 2 and 3. The kinetic reaction of the CPC reactor (1.09) is greater than the ordinary solar reactor (0.34, the intensity of the UV ray in the Reactor 2 go up in the comparison of the intensity of the UV Reactor 3, because of the structure of the CPC that this rise could boost free radical production [24].

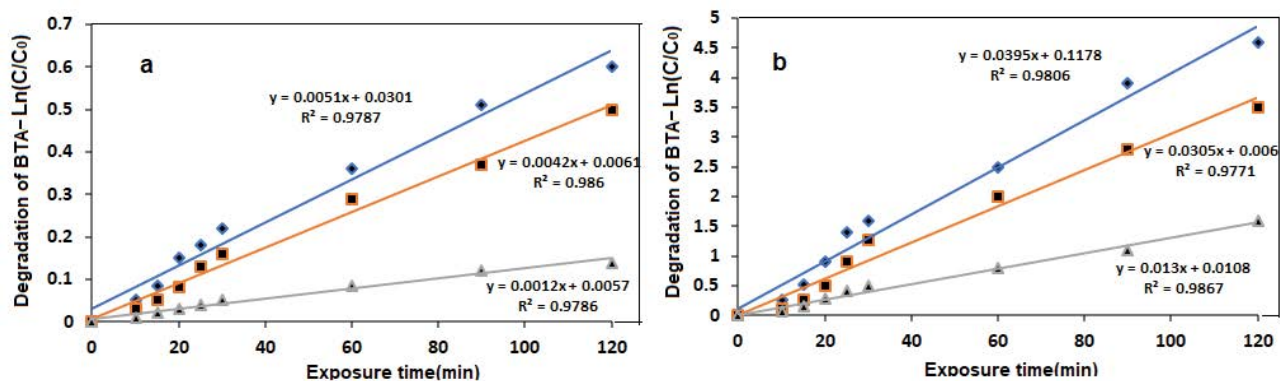


Fig. 7. Reaction kinetics of benzotriazole in photocatalytic degradation (a) and photolysis degradation (b).

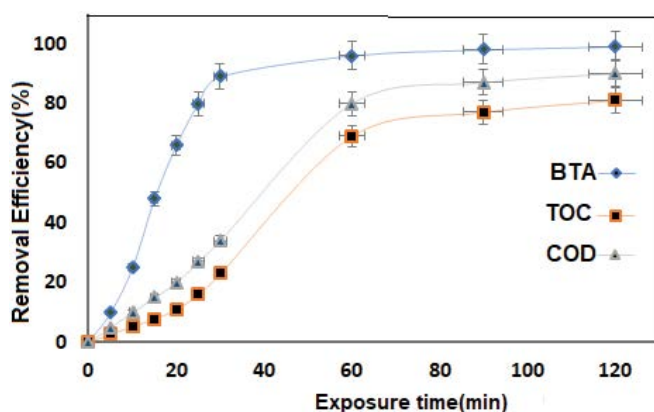


Fig. 8. Rate of the COD and TOC degradation of benzotriazole for photocatalytic degradation

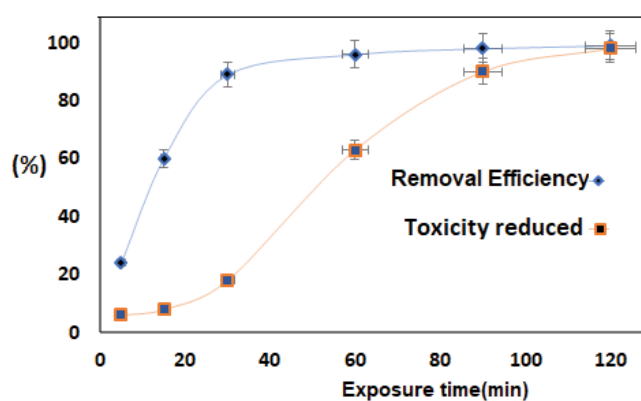


Fig. 9. Acute bio-toxicity evaluations using *Vibrio fischeri* after 48 h of incubation at different benzotriazole concentrations.

3.6. TOC analysis

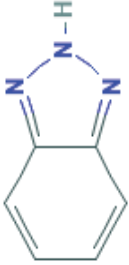
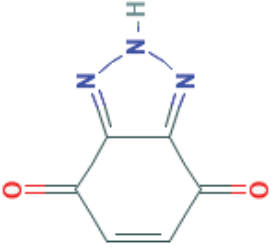
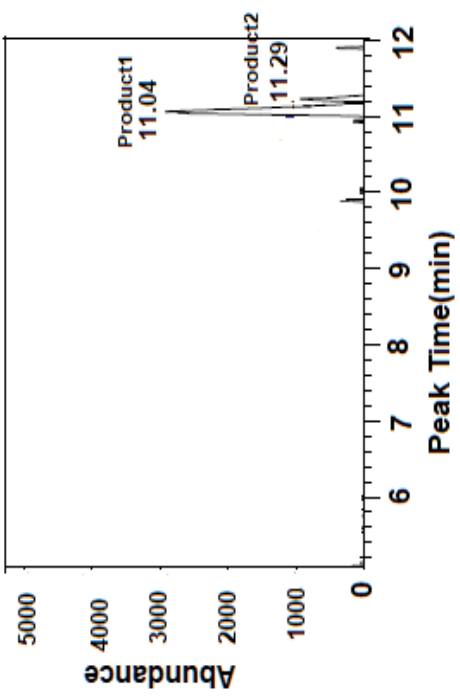
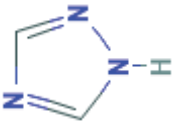
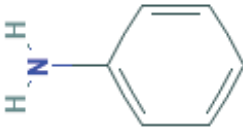
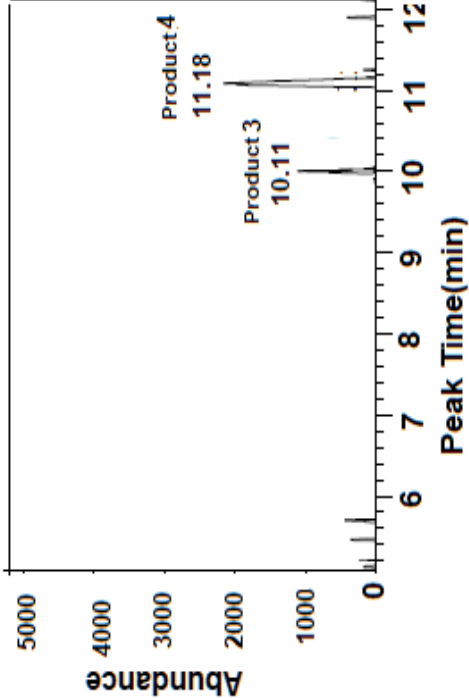
The results of the COD and TOC degradation efficiency of BTA at optimized conditions have been determined in Fig. 8. The amount of the COD degradation of BTA in 15 min 15% reaching 71% in 90 min and reaching 83% at the end of the 120 min and the TOC degradation efficiency started from 12% in 5 min, reaching 85% in 90 min and reaching 90% at the end of the 120 min. The BTA under optimized conditions shows high degradation efficiency and almost completely degraded after 120 min. But COD and TOC removal are slow concerning degradation efficiency. This will be due to the formation of intermediates and later on, these intermediates have been degraded and BTA mineralized after 120 min [20].

3.7. GC-MAS analysis

In the GC-MAS test, samples of the reactors were extracted at times 5, 15, 30, 60 and 120 min. Compounds that were possibly created by the degradation of BTA and indicated by the GC-MAS test in Table and from Product1 to 10 were numbered respectively. The structure of benzotriazole (BT) is based on two fused rings e benzene and thiazole [25,26]. Products after 5–30 min exposure, free radicals

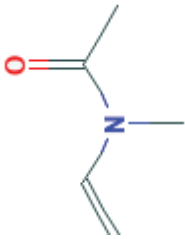
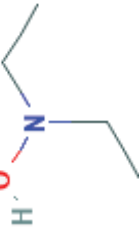
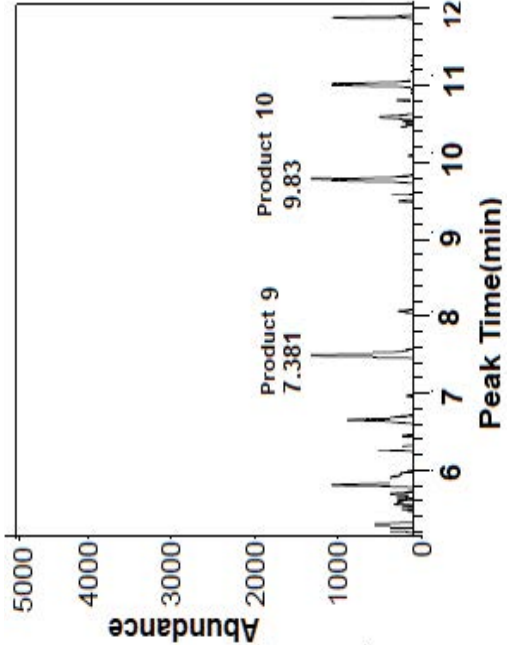
created in the photocatalytic process as OH^\bullet and O^\bullet can cause breaking structures between the C-H, C-N, O-C bonds. As shown in Table 4, in the first reaction, after breaking down the contaminant's structure, materials such as anilin, hydroxybenzotriazole, methyltriazole, and triazole, whose structure is shown in Table (Product1 to 6), which still preserved the circular structure. After 60 min, the materials in contact with free radicals are broken down and form a simpler material that contains mostly of 1H-1,2,4-triazole and 1,2,3-triazolium whose structure is shown in Table 4. After 120 min, the materials in contact with free radicals are broken down and form a simpler material that contains mostly of N-methyl-N-vinyl acetamide and N-diethyl hydroxylamine whose structure is shown in Table 4. Subsequently, the circular structure of these compounds is further converted to simpler materials in contact with OH^\bullet . They had interpreted the reaction mechanism in relation to the photogenerated OH^\bullet radicals and settled that the two compounds are completely converted to by-products that undergo further degradation with the breaking of the triazole ring. Finally, these substances become more stable turning to mineral materials containing nitrate, and ammoniac compound after oxidation. The photocatalytic studies on the BT and BTA decomposition were performed at the irradiance equal to 500 W/m^2 and the following doses of TiO_2 .

Table 4
Molecular structure compounds that were possibly created by the degradation of benzotriazole in GC-MAS test

		By-products after 5 min exposure		GC-MAS	
	Product1	Product2			
Molecular formula					
Proposed structure	$C_6H_5N_3$	$C_6H_3N_3O_2$			
Chemical names	1H-benzotriazole	2H-benzotriazole-4,7-dione			
					
		By-products after 15 min exposure		GC-MAS	
	Product3	Product4			
Molecular formula					
Proposed structure	$C_2H_3N_3$	C_6H_7N			
Chemical Names	Triazole	Aniline			
					

(continued)

Table 4 Continued

By-products after 120 min exposure	
Product9	Product10
	
C_5H_9NO	$C_4H_{11}NO$
N-Methyl-N-vinyl acetamide	N-Diethyl hydroxyl amine
	

The addition of TiO_2 improved considerably the degradation efficiencies of the investigated compounds tolyltriazole, anilin, viny acetamide, and hydroxy amine [25,27]. In another study of the method the photocatalytic studies on the BT and BTA decomposition were performed at the irradiance equal to $500 W/m^2$ and the following doses of TiO_2 : 100, 300, 500 mg/L. The addition of TiO_2 improved considerably the degradation efficiencies of the investigated compounds. After 60 min of the processes performed at the dose of TiO_2 $\frac{1}{4}$ 500 mg/L, the concentrations of both BT and BTA in the reaction solutions were below their LODs. The increase of the reaction rate of BT and BTA photodegradation in the presence of TiO_2 in comparison to the reaction rate of both compounds obtained in the direct photolysis was confirmed by the estimation of the kinetic parameters of these reactions [28]

3.8. Evaluation of BTA and metabolites by using the micro-toxicity test

The benzotriazole contaminant with the effect on *Vibrio fischeri* bacteria in the micro-toxicity test results in limiting the nitrification process. The synthesis process photocatalytic leads to the degradation of BTA and the shatter of this compound into compounds that do not have the inhibitory effect on nitrification and nitrifying bacteria in the micro-test [29,30]. However, with a decrease in benzotriazole by 88%, only 16% of toxicity reduced, which can be attributed to toxic reaction metabolites (Fig. 9). The research showed that, with increasing exposure time of ultraviolet light with the sample containing BTA, the toxicity of the sample was grown, which can be related to the production of toxic metabolites from benzotriazole degradation.

Triazole and aniline are one of the metabolites that are generated less than 1% (0.18 mg/L) in the benzotriazole degradation process, which was not present in the prototype before the contact. Triazolium and phenazine are also a metabolite that is produced in the range of 10%–20%. Studies have shown that toxicity of the phenazine for vibriotic bacterium is 2 times higher than benzothiazole, which EC 50 (15 min) for this compound is 21 mg L (0/122 mmol/L). Nevertheless, the percentages of other metabolite compounds that formed during the degradation of benzotriazole, are from 0.5 to 16%, which are higher molecular weight than benzothiazole and phenazine. The GC-mass data showed two combinations 1,2,3-triazolium and 1H-1,2,4-triazole, which are the result of the metabolization of benzotriazole, which can ascribe the extra toxicity that created by benzotriazole and phenazine in the environment to these two combinations [24]. Aniline and phenazine create yellowish-red and red color in the environment respectively, thus the reason for red color as the result of ultraviolet radiation to benzotriazole can be expressed [24]. Lars et al. with UV degradation of benzotriazole reduced toxicity both in the nitrification test and Microtox. However, while benzotriazole-concentration was reduced with 88%, toxicity was only reduced with 16%. Benzotriazole was obviously transformed into compounds that act toxic for nitrifying bacteria and *V. fischeri*. No effect was observed in the reference sample which leads to the conclusion that the

measured toxicity can be exclusively attributed to benzotriazole and its metabolites [31].

4. Conclusions

The highest photocatalytic and photolysis activity for the degradation of BTA was obtained for the TiO_2/UVc and UV_c whit 99% and 45 efficiencies in 120 min. Also, the highest photocatalytic and photolysis activity for the degradation of BTA has obtained for reactor CPC and 84% and 36% efficiency in 120 min. The photocatalytic degradation reaction of BTA was monitored by HPLC, TOC, and GC-MASS analyses. The GC-MASS analysis results indicate that degradation of BTA occurs through products triazole, tolyltriazole and anilin were identified ring cleavages followed by subsequent reactions with OH radicals. The metabolites show toxic effects, but they are not as toxic as benzotriazole, resulting in a general decrease in toxicity as a result of photocatalytic degradation.

References

- [1] J.W. Frankenfeld, K.U. Ingold, Alkylamine Substituted Benzotriazole Containing Lubricants Having Improved Oxidation Stability and Rust Inhibition (PNE-530), Google Patents, US5076946, 1991.
- [2] Z. Gan, H. Sun, R. Wang, H. Hu, P. Zhang, X. Ren, Transformation of acesulfame in water under natural sunlight: joint effect of photolysis and biodegradation, *Water Res.*, 64 (2014) 113–122.
- [3] S. Weiss, J. Jakobs, T. Reemtsma, Discharge of three benzotriazole corrosion inhibitors with municipal wastewater and improvements by membrane bioreactor treatment and ozonation, *Environ. Sci. Technol.*, 40 (2006) 7193–7199.
- [4] M. Alotaibi, A. McKinley, B. Patterson, A. Reeder, Benzotriazoles in the aquatic environment: a review of their occurrence, toxicity, degradation and analysis, *Water Air Soil Pollut.*, 226 (2015) 226, doi: 10.1007/s11270-015-2469-4.
- [5] M. Ahmadi, K. Rahmani, A. Rahmani, H. Rahmani, Removal of benzotriazole by photo-Fenton like process using nano zero-valent iron: response surface methodology with a Box-Behnken design, *Polish J. Chem. Technol.*, 19 (2017) 104–112.
- [6] H. Rahmani, A. Rahmani, M. Yousefi, K. Rahmani, Degradation of sulfamethoxazole antibacterial by sono-Fenton process using nano-zero valent iron: influence factors, kinetic and toxicity bioassay, *Desal. Water Treat.*, 150 (2019) 220–227.
- [7] S. Nachiappan, K. Muthukumar, Intensification of textile effluent chemical oxygen demand reduction by innovative hybrid methods, *Chem. Eng. J.*, 163 (2010) 344–354.
- [8] A. Yazdanbakhsh, A. Rahmani, M. Massoudinejad, M. Jafari, M. Dashtdar, Accelerating the solar disinfection process of water using modified compound parabolic concentrators (CPCs) mirror, *Desal. Water Treat.*, 57 (2016) 23719–23727.
- [9] M.-R. Zare, M.-M. Amin, M. Nikaen, M. Zare, B. Bina, A. Fatehizadeh, A. Rahmani, M. Ghasemian, Simplification and sensitivity study of Alamar Blue bioassay for toxicity assessment in liquid media, *Desal. Water Treat.*, 57 (2016) 10934–10940.
- [10] N. O'Rourke, L. Hatcher, Factor Analysis and Structural Equation Modeling, SAS Institute, Cary, 2013.
- [11] M. Fazlzadeh, A. Rahmani, H.R. Nasehinia, H. Rahmani, K. Rahmani, Degradation of sulfathiazole antibiotics in aqueous solutions by using zero valent iron nanoparticles and hydrogen peroxide, *Koomesh J. Semnan Univ. Med. Sci.*, 18 (2016) 350–356.
- [12] J. Bandara, J.A. Mielczarski, J. Kiwi, 2. Photosensitized degradation of azo dyes on Fe, Ti, and Al oxides. Mechanism of charge transfer during the degradation, *Langmuir*, 15 (1999) 7680–7687.
- [13] M. Farzadkia, K. Rahmani, M. Gholami, A. Esrafil, A. Rahmani, H. Rahmani, Investigation of photocatalytic degradation of clindamycin antibiotic by using nano-ZnO catalysts, *Korean J. Chem. Eng.*, 31 (2014) 2014–2019.
- [14] M. Gholami, K. Rahmani, A. Rahmani, H. Rahmani, A. Esrafil, Oxidative degradation of clindamycin in aqueous solution using nanoscale zero-valent iron/ H_2O_2 /US, *Desal. Water Treat.*, 57 (2016) 13878–13886.
- [15] K. Sivagami, R.R. Krishna, T. Swaminathan, Photocatalytic degradation of pesticides in immobilized bead photoreactor under solar irradiation, *Sol. Energy*, 103 (2014) 488–493.
- [16] K. Sunada, T. Watanabe, K. Hashimoto, Studies on photokilling of bacteria on TiO_2 thin film, *J. Photochem. Photobiol., A*, 156 (2003) 227–233.
- [17] A.V. Emeline, V.N. Kuznetsov, V.K. Rybchuk, N. Serpone, Visible-light-active titania photocatalysts: the case of N-doped TiO_2 s—properties and some fundamental issues, *Int. J. Photoenergy*, 2008 (2008) 258394, doi: 10.1155/2008/258394.
- [18] S. Sato, R. Nakamura, S. Abe, Visible-light sensitization of TiO_2 photocatalysts by Et-method N doping, *Appl. Catal., A*, 284 (2005) 131–137.
- [19] Y.Y. Gurkan, N. Turkten, A. Hatipoglu, Z. Cinar, Photocatalytic degradation of cefazolin over N-doped TiO_2 under UV and sunlight irradiation: prediction of the reaction paths via conceptual DFT, *Chem. Eng. J.*, 184 (2012) 113–124.
- [20] E. Felis, A. Sochacki, S. Magiera, Degradation of benzotriazole and benzothiazole in treatment wetlands and by artificial sunlight, *Water Res.*, 104 (2016) 441–448.
- [21] R. Andreozzi, V. Caprio, A. Insola, G. Longo, Photochemical degradation of benzotriazole in aqueous solution, *J. Chem. Technol. Biotechnol.*, 73 (1998) 93–98.
- [22] F.J. Benitez, J.L. Acero, F.J. Real, G. Roldan, E. Rodriguez, Photolysis of model emerging contaminants in ultra-pure water: kinetics, by-products formation and degradation pathways, *Water Res.*, 47 (2013) 870–880.
- [23] S. Bahn Müller, C.H. Loi, K.L. Linge, U. von Gunten, S. Canonica, Degradation rates of benzotriazoles and benzothiazoles under UV-C irradiation and the advanced oxidation process $\text{UV}/\text{H}_2\text{O}_2$, *Water Res.*, 74 (2015) 143–154.
- [24] L.J. Hem, T. Hartnik, R. Roseth, G.D. Breedveld, Photochemical degradation of benzotriazole, *J. Environ. Sci. Health., Part A*, 38 (2003) 471–481.
- [25] V. Matamoros, Y. Rodríguez, J. Albaigés, A comparative assessment of intensive and extensive wastewater treatment technologies for removing emerging contaminants in small communities, *Water Res.*, 88 (2016) 777–785.
- [26] V. Matamoros, E. Jover, J.M. Bayona, Occurrence and fate of benzothiazoles and benzotriazoles in constructed wetlands, *Water Sci. Technol.*, 61 (2010) 191–198.
- [27] J.S. Miller, D. Olejnik, Photolysis of polycyclic aromatic hydrocarbons in water, *Water Res.*, 35 (2001) 233–243.
- [28] E. Felis, A. Sochacki, S. Magiera, Degradation of benzotriazole and benzothiazole in treatment wetlands and by artificial sunlight, *Water Res.*, 104 (2016) 441–448.
- [29] M.-R. Zare, M.-M. Amin, M. Nikaen, B. Bina, A. Rahmani, S. Hemmati-Borji, H. Rahmani, Acute toxicity of Hg, Cd, and Pb towards dominant bacterial strains of sequencing batch reactor (SBR), *Environ. Monit. Assess.*, 187 (2015) 263, doi: 10.1007/s10661-015-4457-y.
- [30] A. Rahmani, A. Asadi, A. Fatehizadeh, A.R. Rahmani, M.R. Zare, Interactions of Cd, Cr, Pb, Ni, and Hg in their effects on activated sludge bacteria by using two analytical methods, *Environ. Monit. Assess.*, 191 (2019) 124, doi: 10.1007/s10661-019-7241-6.
- [31] L.J. Hem, T. Hartnik, R. Roseth, G.D. Breedveld, Photochemical degradation of benzotriazole, *J. Environ. Sci. Health. Part A Toxic/Hazard. Subst. Environ. Eng.*, 38 (2003) 471–481.